

# We are IntechOpen, the world's leading publisher of Open Access books Built by scientists, for scientists

6,900

Open access books available

185,000

International authors and editors

200M

Downloads

Our authors are among the

154

Countries delivered to

TOP 1%

most cited scientists

12.2%

Contributors from top 500 universities



WEB OF SCIENCE™

Selection of our books indexed in the Book Citation Index  
in Web of Science™ Core Collection (BKCI)

Interested in publishing with us?  
Contact [book.department@intechopen.com](mailto:book.department@intechopen.com)

Numbers displayed above are based on latest data collected.  
For more information visit [www.intechopen.com](http://www.intechopen.com)



---

# Performance Evaluation of Nanostructured Solar Cells

---

Abouelmaaty M. Aly

Additional information is available at the end of the chapter

<http://dx.doi.org/10.5772/67405>

---

## Abstract

Nanotechnology is making great contributions in various fields including harvesting solar energy through solar cells since nanostructured solar cells can provide high performance with lower fabrication costs. The transition from fossil fuel energy to renewable sustainable energy represents a major technological challenge for the world. The solar cells industry has grown rapidly in recent years due to strong interest in renewable energy in order to handle the problem of global climate change that is now believed to occur due to the use of fossil fuels. Cost is an important factor in the eventual success of any solar technology since inexpensive solar cells are needed to provide electricity especially for rural areas and for underdeveloped countries. Therefore, new developments in nanotechnology may open the door to the production of cheaper and more efficient solar cells by reducing the manufacturing costs of solar cells. This chapter covers a review of the progress that has been made to-date to enhance efficiencies of various nanostructures used in solar cells including utilizations of all the wavelengths present in of the solar spectrum.

**Keywords:** nanostructured solar cells, power efficiency, quantum wells, quantum wires, quantum dots, intermediate bands, solar concentrations

---

## 1. Introduction

The worldwide demand for energy has an environmental impact on the global climate since most of the energy in recent decades has come from the combustion of fossil fuels. Many technologies are being considered to supplement this energy such as renewable energy sources (RESs). RESs are the key to long-term solution of industrialized economies from complete dependence on fossil fuels [1]. Solar energy conversion is the most attractive source of RESs because solar energy is abundant and it is free. In the past 50 years, silicon (Si) solar cells (SCs) have been developed

with demonstrated efficiency of nearly 25%, which is very close to the theoretical limit for a single junction under one sun concentration of  $\sim 31\%$  [2]. Unfortunately, this type of bulk Si SCs is too expensive for mass production. For the solar energy conversion, Si is not the ideal material because the indirect bandgap of Si has a significant negative impact on the optical absorption [1]. As a result, the 90% of sunlight is absorbed when the energy of photons is greater than the bandgap of Si and the thickness of Si is around  $125\ \mu\text{m}$ , whereas for a direct bandgap material such as gallium arsenide (GaAs), the required thickness is around  $0.9\ \mu\text{m}$  [3]. In addition, the incoming photons on the bulk Si SCs should have the same energy of the bandgap of Si to obtain a free electron. The photon will have dissipated inside the bulk Si, if it has energy less than bandgap of Si. If it has more energy than bandgap of Si, the extra energy will be lost as heat. These factors cause the loss of around 70% of the radiation energy incident on the cell [4]. This trade-off between the two factors is evident from the current density-voltage ( $J$ - $V$ ) curves shown in **Figure 1(a)** for some elemental semiconductors, such as germanium (Ge) or Si, and binary compounds, such as GaAs, aluminium antimonide (AlSb) and gallium phosphide (GaP). The main problem of the bulk SCs is evident in **Figure 1(a)** in that when the output current increases the output voltage decreases and vice versa based on bandgap energies of these materials. Therefore, the optimum bandgap energy of SC matches the maximum efficiency can be calculated as shown in **Figure 1(b)**. This figure shows the maximum efficiency versus bandgap energy of bulk SCs under Blackbody spectrum and more realistic AM0 and AM1.5 solar spectra at one sun and maximum concentrations.

Nanotechnology is an important vehicle to reduce the SC cost and to improve its performance by utilizing nanostructured materials in SCs [6]. Nanostructured materials are generally defined as those materials whose structural elements (crystallites or molecules) have dimensions in the 1–100 nm range. Attention of both academic and industrial researchers for these materials over the past decade arises from the remarkable differences in fundamental electrical, optical and magnetic properties that occur with change in size while controlling the construction of the materials at the atomic level. The motivation for using nanostructured materials emerges from their specific physical and chemical properties. Enhancing the regular crystalline structure using nanocrystalline materials in the form of thin films or multi-layers SCs can increase the absorbance of all incident solar spectra [7, 8]. In nanoparticle-based SCs, the particles should be sufficiently close to one another to transfer the charges directly. Recently, significant progress has

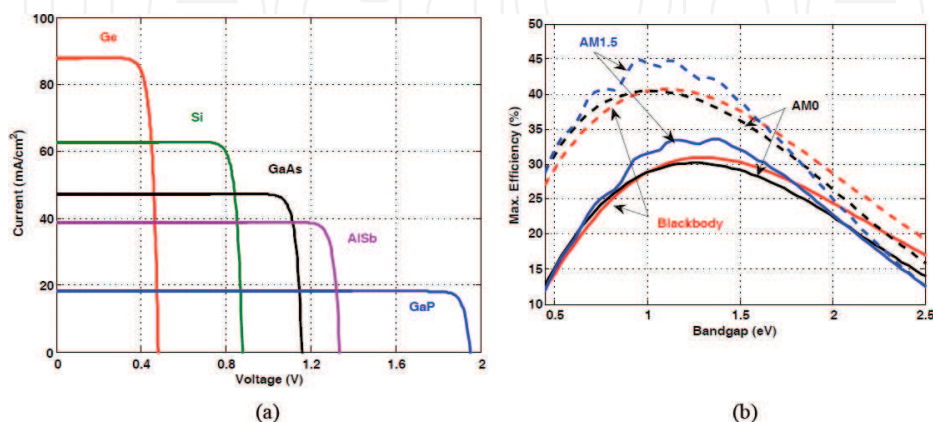


**Figure 1.** (a)  $J$ - $V$  curves of some semiconductors for bulk SCs and (b) maximum efficiencies versus bandgap energies of bulk SCs with different spectra at one sun (solid lines) and maximum concentration (dashed lines) [5].

been made in improving the overall efficiencies of SC structures, including the incorporation of potential well and nanocrystalline materials. The present investigation deals with some potential applications of nanostructured materials in solar energy conversion and to give an overview on current research topics in this field. This chapter includes the following sections: preparation of SCs in Section 2; fundamental of nanostructure confinement in Section 3; nanostructures for SC applications in Section 4 and conclusions in Section 5.

## 2. Preparation of solar cells

Over the past 20 years, electrical power generation output of SCs has grown up to  $5 \times 10^9$  W (5 GW). This is still small in comparison to the world total electric generation capacity of  $4 \times 10^{12}$  W (4 TW) although it represents a large step forward in this promising renewable energy technology [9]. If the present rate of growth continues, solar energy could become the dominating power generation method by the end of this century. The first generation of SCs comprises technologies where the photon absorber is a thin *p*-doped single crystal Si wafer. Employing Si in the form of monocrystalline or polycrystalline material for this purpose is understandable in view of its abundance, stability, non-toxicity and decades of industry experience. However, single-crystal Si wafers are very expensive to produce due to the demands of high purity and high accuracy of sawing a single wafer from Si. The proposed practical bound on cell efficiency under one sun has been estimated to be about 25%. The second generation of SCs aims at reducing the costs of producing thin-film SCs by growing thin layers of Si and other semiconductors on glass substrates. This generation of SCs uses materials, such as cadmium telluride (CdTe), copper-indium-gallium selenide (CIGS), copper-indium sulphide (CIS) and amorphous Si (a-Si). These materials are much cheaper than using a single-crystal Si but have the downside of leading to less efficient SCs with efficiency around 16% due to structural defects [10]. The third generation of SCs is made from variety of new materials besides Si to make solar energy more efficient over a wider band of solar energy including IR band. There are several technologies in this generation based on nanotechnology such as hot carrier, tandem or multi-junction, and intermediate-band SCs. The best overall efficiency for this generation has reached to 44.7% at one sun. Research into the fourth generation of SCs has recently begun, and they are made from hybrid organic materials, which are low cost and nanostructure inorganic materials with stable lifetime. This technology could significantly improve the harvesting and conversion of solar energy [11]. This generation of materials could improve the efficiency while maintaining their low cost when compared to third-generation materials.

## 3. Fundamentals of nanostructure confinement

This section gives an overview of the optical properties of quantum-confined semiconductor structures. The potential barriers in these artificial structures can confine the motion of electrons and holes (charge carriers, CCs) in one or more directions [12]. The optical properties of bulk solids do not usually depend on their size. For example, ruby crystals have the

same red colour regardless of how big they are [13]. This statement is only true as long as the dimensions of the crystal are large. For very small crystals, the optical properties are dependent on the size such as semiconductor-doped glasses. These contain very small semiconductor micro-crystals within a colourless glass, and the colour of the filter can be altered just by changing the size of the crystals. The amount of dependence of optical properties in very small crystals is the result of the quantum confinement effect. The bulk crystal will not exhibit any quantum size effects. To observe quantum size effects, the layers should be thin. The general scheme for classifying quantum-confined structures is given in **Table 1**. The artificial structures are classified as to whether the CCs are free or confined in one, two or three dimensions. For bulk semiconductors, the CCs are free (not confined) to move within their respective bands in all the three directions. For quantum-confined semiconductors, the structures are respectively called quantum wells (QWs) for confinement in one-dimensional (1D), quantum wires (QRs) for confinement in two-dimensional (2D) and quantum dots (QDs) for confinement in three dimensions (3D). The nanocrystal dimensions required to observe quantum-confinement effect, have to be produced by the advanced techniques such as advanced epitaxial crystal growth (QW structures), epitaxial growth on patterned substrates (QR structures) and spontaneous growth technique (QDs structures) [12].

In a nanocrystalline particle with dimensions  $L_x$ ,  $L_y$  and  $L_z$ , the CCs are localized in the region with the minimum potential energy in the nanoparticle, and its energy spectrum is no longer formed from allowed and forbidden bands as in crystals, but from discrete levels as shown in **Figure 2(a)** and given by [14]:

$$E(k_x, k_y, k_z) = E_c + \frac{\hbar^2}{2m} \left( \frac{p\pi}{L_x} \right)^2 + \frac{\hbar^2}{2m} \left( \frac{q\pi}{L_y} \right)^2 + \frac{\hbar^2}{2m} \left( \frac{r\pi}{L_z} \right)^2 = E_{pqr} \quad (1)$$

Here  $\hbar$  is the Planck's constant,  $m$  is the effective mass,  $E$  is the total energy of CCs,  $k$  is the wave-vector,  $E_c$  is the edge energy of CCs in the conduction band (CB) or valence band (VB), and  $p$ ,  $q$  and  $r$  are integer numbers. These discrete levels result from the Schrödinger Equation satisfied by the CCs in the materials [15]. A discrete energy spectrum is similar to that in atoms or molecules. A nanoparticle is called QD if the discrete energy levels can be observed, that is, if the difference between adjacent discrete energy levels is higher than the thermal vibration energy,  $k_B T$  as  $T$  is the temperature and  $k_B$  is the Boltzmann constant. This implies that  $\hbar^2 \pi^2 / 2m L_x^2$ ,  $\hbar^2 \pi^2 / 2m L_y^2$  and  $\hbar^2 \pi^2 / 2m L_z^2$  are higher than  $k_B T$  or  $L_x, L_y, L_z < \sqrt{\hbar^2 \pi^2 / 2m k_B T}$ .

In a QD, the CCs are not free to move because it is localized in the dot. There are also structures in which CCs movement is allowed along a single direction, that is, QRs, or in one plane, that is, QWs. Unlike these structures, in a bulk crystalline material the CCs can freely move along all three spatial directions and the energy dependence on the  $k$  and it is given by

$$E(k) = E_c + \hbar^2 k^2 / 2m = E_c + \hbar^2 (k_x^2 + k_y^2 + k_z^2) / 2m \quad (2)$$

**Figure 2(b)** shows a QR with  $L_y$  and  $L_z$  dimensions along the confinement directions. The CCs can freely move along only the  $x$ -direction and the dispersion relation is expressed as

$$E(k_x, k_y, k_z) = E_c + \frac{\hbar^2}{2m} \left( \frac{q\pi}{L_y} \right)^2 + \frac{\hbar^2}{2m} \left( \frac{r\pi}{L_z} \right)^2 + \frac{\hbar^2 k_x^2}{2m} = E_{s,qr} + \frac{\hbar^2 k_x^2}{2m} \quad (3)$$

Structure	Quantum confinement	Dimensionality
Bulk	None	3
QW	1D	2
QR	2D	1
QD	3D	0

**Table 1.** Classification of quantum-confined structures.

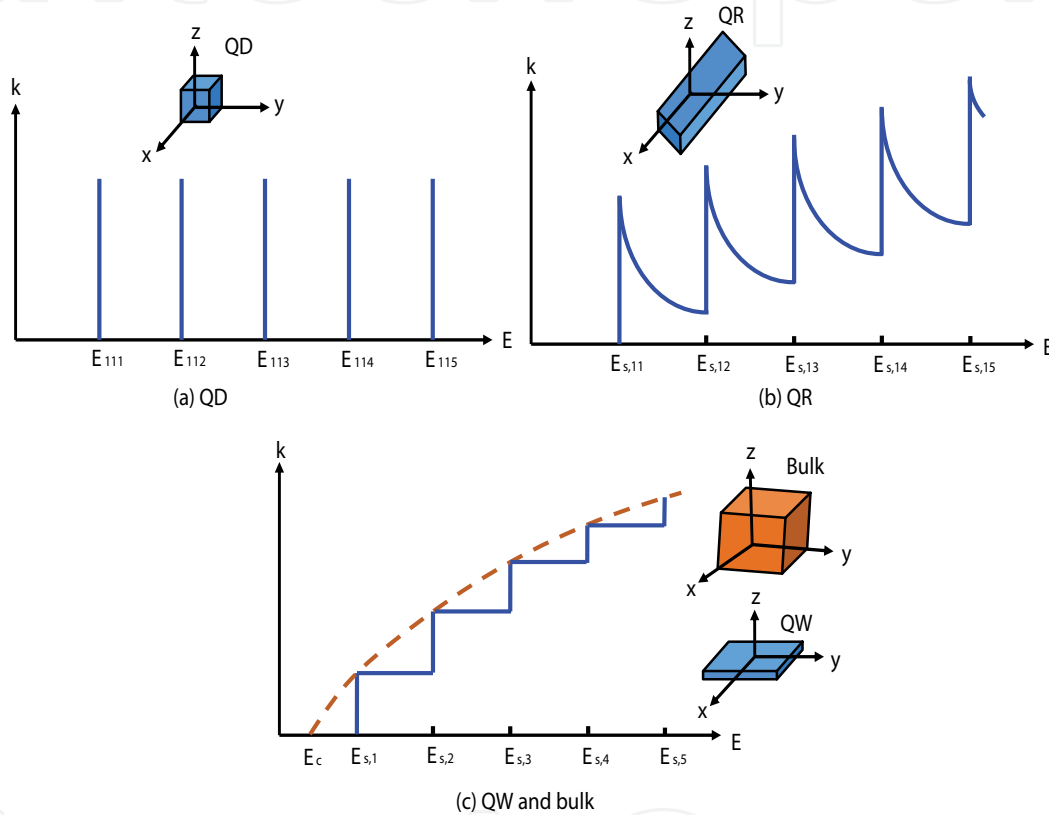


**Figure 2.**  $E$ - $k$  relations for QD, QR, and QW and bulk crystalline lattices. (a) QD, (b) QR and (c) QW and bulk.

As in a QD, the difference between adjacent discrete levels must be higher than  $k_B T$ , that is,  $L_y, L_z < \sqrt{\hbar^2 \pi^2 / 2m k_B T}$ .

Analogously, in a QW as shown in **Figure 2(c)**, the CCs are free to move along the  $x$  and  $y$  directions and the dispersion relation is

$$E(k_x, k_y, k_z) = E_c + \frac{\hbar^2}{2m} \left( \frac{r\pi}{L_z} \right)^2 + \frac{\hbar^2(k_x^2 + k_y^2)}{2m} = E_{s,r} + \frac{\hbar^2(k_x^2 + k_y^2)}{2m} \quad (4)$$

These discrete energy levels can be observed if the width of the QW satisfies the relation  $L_z < \sqrt{\hbar^2 \pi^2 / 2m k_B T}$ . The dashed line in **Figure 2(c)** represents the density of  $k$  versus  $E$  in a bulk crystalline lattice as the CCs freely move in three dimensions and is given by the equation  $E = \hbar^2 k^2 / 2m$ .

In QWs, QRs and QDs, the allowed region in which the CCs move is called *potential well*, and the region where this motion is forbidden is referred to as *potential barrier*. The excitation of an electron from the VB to CB as a result of photon absorption is only possible if the photon energies ( $E$ ) are higher than the bandgap energy ( $E_g$ ) of the material that contains the QW (for example); this minimum photon energy also depends on the width of the well and the height of the potential barrier as shown in **Figure 3(a)**.

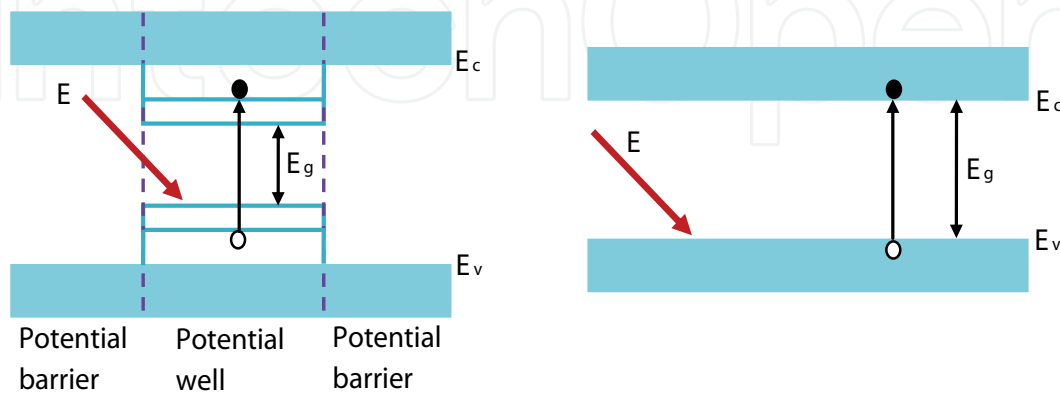


**Figure 3.** Construction of energy band diagram for two semiconductor material.

More precisely, the electron transition from the VB with upper edge ( $E_v$ ) to the CB with bottom edge ( $E_c$ ) occurs between the corresponding discrete levels in the *potential well*. In bulk crystals, the similar electron excitation occurs if the incident photon energy  $E$  is equal to  $E_g$ , as shown in **Figure 3(b)**. The absorption spectrum depends on the nanoparticle diameter due to the above relations between the CC energy and the dimensions of the *potential well*. When several QWs, QRs or QDs are separated by small distances, the CCs can jump from one structure to another if their energy (thermal) is high enough to overcome the potential barrier.

#### 4. Nanostructures for solar cell applications

With improved possibilities for the control of material texture on the nm scale, nanostructured SCs have received increased scientific attention in recent years. Nanostructures can allow efficient SCs to be made from cheaper materials, such as Si and titanium dioxide ( $\text{TiO}_2$ ) [16]. Although there will be cost barriers involved in developing mass production techniques for nanostructured SCs, the use of cheaper raw materials will allow a cost reduction of commercial SCs. Nanomaterials and nanostructures hold promising possibilities to enhance the performance of SCs by improving both optical absorption and photo-carrier collection. Meanwhile, the new materials and structures can be fabricated in a low-cost fashion, enabling cost-effective production of SCs. As the performance of SCs largely depends on the above two factors, they have to be optimized for SCs with suitable energy conversion efficiency. Nevertheless, the requirements in optimizing these factors can be in conflict. For example, in a planar-structured SC thicker materials are needed in

order to achieve sufficient optical absorption; however, it will reduce carrier collection probability due to the increased minority carrier diffusion path length and vice versa. In fact, recent studies have shown that nanostructures not only improve optical absorption by utilizing the light trapping effect but also facilitate the photocarrier collection through perpendicular directions of light propagation and carrier collection. The nanostructures discussed in the following sections are classified into four types: nanocomposites, QWs, QRs and QDs.

#### 4.1. Nanocomposites materials for solar cells

Nanocomposites and nanostructured materials are now being investigated for their potential applications in SCs. In nanoparticles of diameter,  $d$ , the number of atoms residing on their surfaces varies as  $1/d$  and hence they can become significant fractions of the atoms present in the core of the few nm size nanoparticles. In such a case, the surface interactions control the behaviour of nanoparticles. Therefore, these small particles often have different characteristics and properties than larger pieces of the same material. Nanostructured layers in thin film SCs offer a number of important advantages [17]: (i) due to multiple reflections, the effective optical path for absorption is much larger than the actual film thickness and (ii) light-generated CCs need to travel over a much shorter path and thus recombination losses are greatly reduced. As a result, the absorber layer thickness in nanostructured SCs can be as thin as 150 nm instead of several micrometres in the conventional thin film SCs and thus reduced installation costs achieved; (iii) the energy bandgap of various layers can be designed to the desired value by varying the size of nanoparticles and (iv) reduced manufacturing costs as a result of using a low-temperature process instead of the high-temperature vacuum deposition process for conventional SCs. Thin films of polycrystalline CdTe, cadmium selenide (CdSe) and cadmium sulphide (CdS) have been reported as the most promising photovoltaic materials for thin film SCs [16]. Other types of nanostructured materials used for SC applications are the hot carrier SCs (HCSCs) and the dye-sensitized SCs (DSSCs).

In a HCSC, the rate of photo-excited carrier is slow enough to allow time for the carriers to be collected and thus allowing higher voltages to be achieved from the cell [18]. The bulk cell is designed to collect the CCs before the hole and the electron recombined while the hot carrier cell catches CCs before the carrier cooling stage. For the HCSC to be effective, CCs should be collected from the absorber over a very small energy range. Hence, special contacts are used to prevent the contacts from cooling the carriers. The limiting efficiency of this approach can reach 86.8%, which is same as an infinite tandem cell stack. However, in order to achieve this limiting efficiency, carrier cooling rates should be reduced or radiative recombination rates should be accelerated [19].

Developing a hot carrier absorber material, which exhibits sufficiently slow carrier cooling to maintain a hot carrier population under realistic levels of sun concentration, is a key challenge. A candidate for the absorber material is a QD super-lattice [20]. InGaAs/gallium arsenide phosphide (GaAsP) is proposed as a suitable absorber material and the GaAs surface buffer layer was reduced in thickness to maximize photon absorption in the well region. An enhanced hot carrier effect was observed in the optimized structures. The HCSC with indium nitride (InN) absorber layer gives a highest efficiency of 52% as shown in **Figure 4** [21]. The efficiency of the HCSC, with

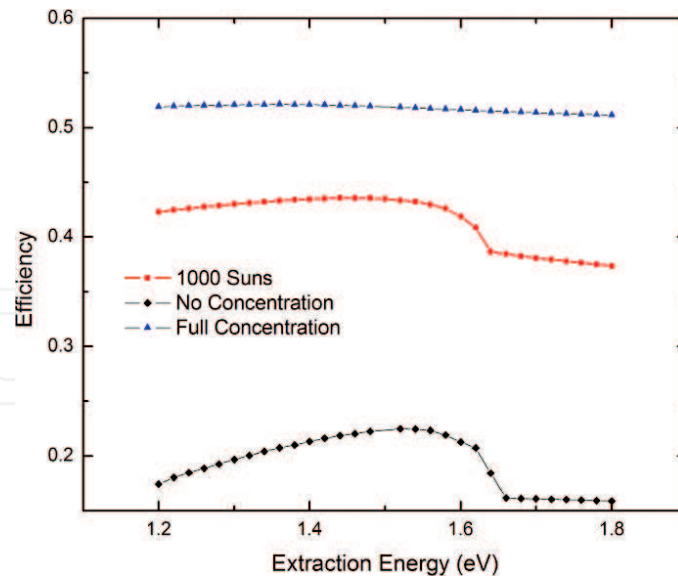


**Figure 4.** HCSC efficiency versus carrier extraction energy with absorber layer (InN) thickness = 50 nm at different sun concentrations [21].

gallium antimonide (GaSb)-based heterostructures as absorber candidates, is improved significantly compared to a fully thermalized single *p-n* junction of similar bandgap energy.

A DSSC is a type of photoelectrochemical SC [22]. In a DSSC, dye molecules are used to sensitize wide-bandgap energy semiconductors ( $\sim 3.2$  eV), such as  $\text{TiO}_2$  and ZnO, which assist in separating electrons from photo-excited dye molecules. These materials are very inexpensive compared to expensive Si or III-V group semiconductors. As a result, much cheaper solar energy at \$1 or less per peak Watt (\$1/pW) can be achieved [23]. The DSSC involves a set of different layers of components stacked in serial. Incoming photons excite electrons in the dye which are efficiently captured by the  $\text{TiO}_2$  and transported to the anode [24]. On the other side, an electrolyte ( $\text{I}^-/\text{I}_3^-$ ) replenishes the electrons in the dye (i.e.  $3\text{I}^- = \text{I}_3^- + 2\text{e}^-$ ), and thus completes the flow of current through the cathode. In order to maximize the contact area between the wide-bandgap energy semiconductors and the dye, it is advantageous to have the wide-bandgap energy semiconductors in the form of nanoparticles or nanotubes. In combination with new absorbing molecules, such structures have helped to improve the performance of DSSCs.

**Figure 5** uses carbon nanotube (CNT) fibres, which have been used as a conductive material to support the dye-impregnated  $\text{TiO}_2$  nanoparticles. Since  $\text{TiO}_2$  nanoparticles present in CNTs are capable of injecting electrons from their excited state and therefore separation and flow of the charges are improved. CNTs are also popular materials for DSSC counter electrode (cathode) fabrication. In addition to enhance conversion efficiency, the cells with CNT counter electrode are expected to provide several advantages including nanoscale conducting channels, lightweight and low cost, as well as improved mechanical properties and thermal stability [25]. Since the invention of the DSSCs in 1990, efficiency has improved from  $\sim 2\%$  to  $\sim 12\%$ . It has a major cost advantage over bulk Si SCs. Some of the main drawbacks of DSSCs are the use of liquid electrolyte and dyes, long-term lifetime and degradation [26]. Most DSSCs use the organic dyes, which have large optical absorption in the visible range

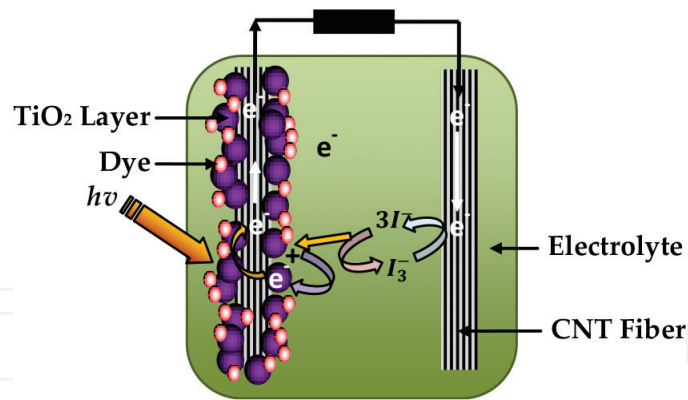


Figure 5. Wire-shaped DSSC made from two CNT fibres.

of 300–700 nm but weak absorption in the IR spectrum. Searching for new materials with absorption spectra extending into the IR range is decisive for enhancing the performance of SCs. A promising alternative for broadband solar absorbers will be inorganic semiconductor sensitizers. In 2013, the performance of semiconductor-sensitized SCs (SSSCs) was improved and the efficiency has increased from 12% to 15% [23]. Inorganic semiconductor sensitizers have several advantages over organic dyes such as tunable absorption bands due to the quantum-size effect and multi-electron-hole pair generation by a single incident photon.

#### 4.2. Quantum well solar cells

Since several decades, QWs have been studied for the application in electronics and photonics. They confine the CCs in 1D and create a sheet of CCs with well-defined energy levels and high mobility due to adjustment in the band structure [1]. Recently, concerted efforts for the manufacture of SCs by incorporating multi-QWs (MQWs) with lower bandgap energy in the active region of the device were carried out. In the beginning, MQWs depended on the III-V semiconductor materials, mainly GaAs and related alloys such as AlGaAs and InGaAs [27]. The main expected benefit of such SCs is high short circuit current due to the enhanced absorption. **Figure 6** shows a structure of GaAs *p-i-n* SC with a single InGaAs QW in intrinsic region [28]. In this work, a short circuit current density is an enhancement, as the absorption in QWs is very high due to the carrier density obtained by quantum confinement in the plane of the well. On the other hand, there is often a corresponding reduction in the open circuit voltage due to the inclusion of lower bandgap energy material which could be overcompensated through the increase in short circuit current from the QWs. GaAs SCs currently hold the world efficiency record for single junction SCs. MQW solar cells (MQWSCs) can achieve optimal bandgap energies for the highest single-junction efficiencies due to the tunability of the QW width and composition. However, the increase in the number of QWs causes mismatch in the lattice and, therefore, disorder occurs in the open circuit voltage [29]. In reference [28], strain-balanced GaAsP/InGaAs MQW in *i*-region has been studied. The GaAsP/InGaAs MQW strain-balanced SC (SB-QWSC) has shown an extraordinary performance for the MQW cell design, achieving high efficiency. The dependence of conversion efficiency on indium (In) and phosphide (P) compositions is examined in **Figure 7** for 20 layers of QWs.

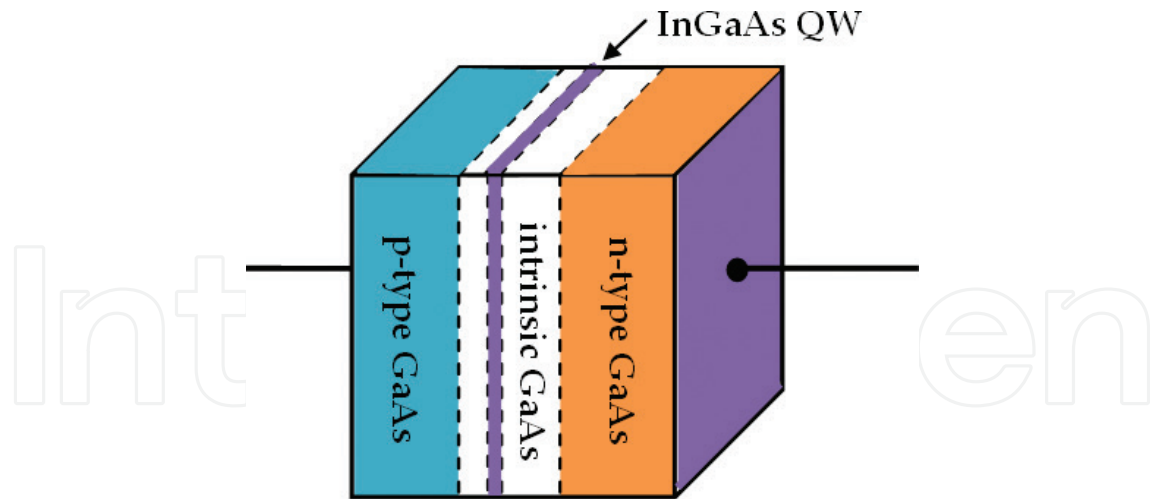


Figure 6. GaAs *p-i-n* SC with a single InGaAs QW in *i*-region.

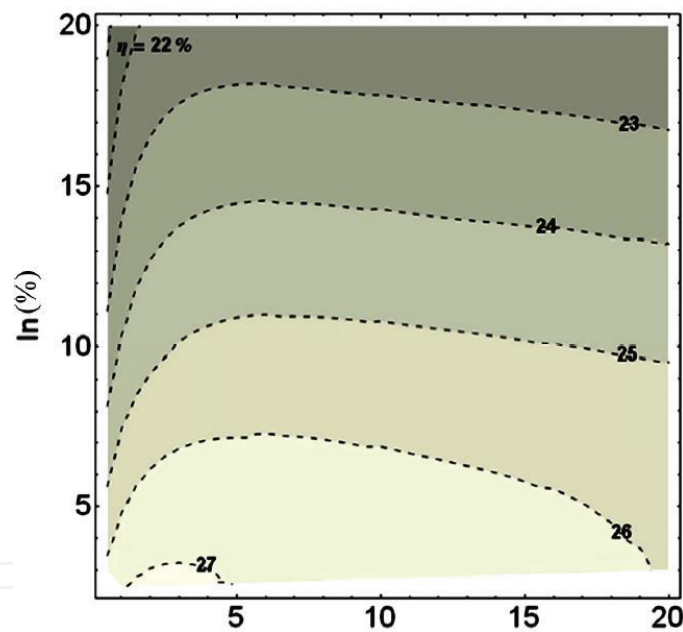


Figure 7. Contour plot for conversion efficiency ( $\eta$ ) versus In and P compositions for 20 layers of QWs and each with thickness of 15 nm [28].

Each well has thickness of 15 nm. In and P compositions are varied in the range from 0.5% to 20% during the development process of the contour plot. It is evident that the highest efficiency equals 27%. This occurs at a composition of not greater than 3% and 5%, respectively, for In and P.

#### 4.3. Quantum wires solar cells

A number of researchers proposed to use QRs in all inorganic structures to produce SCs with both improved efficiency as well as greater stability compared to organic SCs [30, 31]. These

structures include vertical arrays of radial or axial  $p$ - $n$  junction QRs to confine the CCs in 2D and to enhance photon absorption, see **Figure 8**. The radial geometry offers a large area of the depletion region along the QRs and a small QRs volume combined with short carrier diffusion lengths before collection at the contacts as a usable current. The axial geometry offers greater flexibility with respect to materials combinations. Challenges for both architectures are overcoming the barrier of single to tandem junction performance and limitations of surface recombination which leads to loss of CCs.

The potential for improved performance and cost reductions of QR arrays over their bulk SCs is mainly due to (i) increased absorption due to diffuse light scattering in QR arrays; (ii) short collection lengths of minority carriers that are radially separated and (iii) flexibility of cell integration on a variety of low-cost carrier substrates [30]. Recently, the nanostructure of Si QRs has attracted great attention because of its excellent anti-reflection and light trapping effect [32]. This structure is a candidate to lower both the required quality and quantity of Si material. Many researchers have investigated Si QRSCs to provide support for further improvement. However, the efficiency of Si QRSCs still falls behind that of the bulk crystalline Si SCs as a result of the limitation of the extremely high surface recombination in Si QRs. The repression of carrier recombination in Si QRs turns out to be the primary focus for the performance improvement of Si QRSCs. Surface passivations, such as thermal oxidation, carbon thin films and chlorine dielectric treatment, have been widely studied to improve the electrical characteristics of Si QRSCs [33]. These techniques can only work on the recombination at the Si QRs surface. However, a recent attempt has demonstrated that, in addition to the surface recombination, high Auger recombination near the surface plays a key role in the limitation of the photogenerated carrier collection and cell efficiency in Si QRSCs [32]. The Auger recombination comes from the high doping related to in-diffusion through the large surface area of the Si nanostructure. This near surface Auger recombination grows over the surface recombination, especially for the excessive doping condition in Si QRSCs.

In order to reduce recombination both at and near the surface in Si QRs while maintaining good light trapping, an efficient method of Si nitride ( $\text{SiN}_x$ ) passivation is proposed [34].  $\text{SiN}_x$  can provide not only effective surface passivation but also bulk passivation because of the hydrogen diffusion which effectively reduces defect state density and suppresses the Auger recombination at and near the surface [35]. Also, to obtain the best recombination repression both at and near the

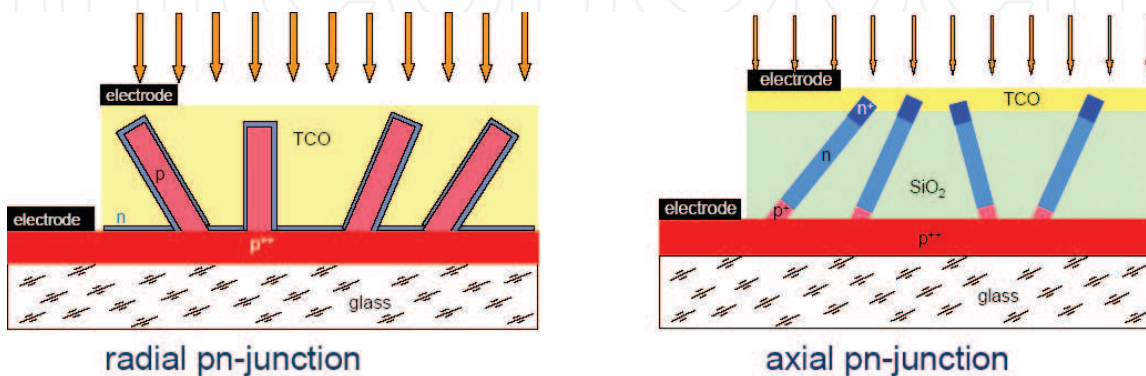


**Figure 8.** Two structures of QRSCs.

surface, another work proposed for surface passivation uses  $\text{SiN}_x$  combined with the Si dioxide ( $\text{SiO}_2$ ). The  $\text{SiO}_2/\text{SiN}_x$  stack performs better due to the more homogeneous Si- $\text{SiO}_2$  self-oxidation interface as well as decreases surface state density [34]. The current-voltage characteristics of Si QRSC passivated with different materials that were measured under illumination conditions of AM1.5G are shown in **Figure 9**.

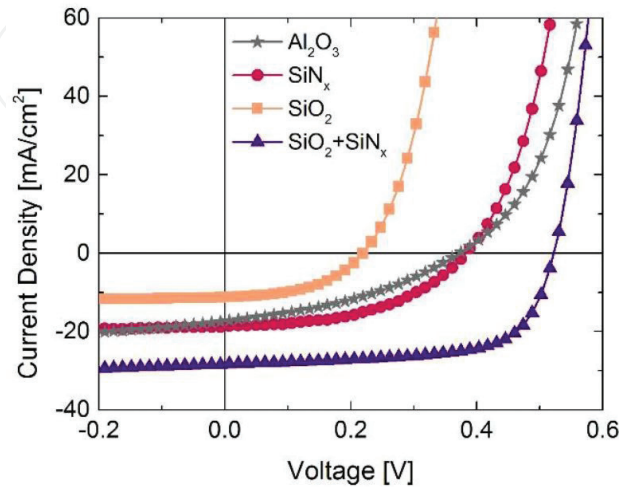


**Figure 9.** Current-voltage characteristics under AM1.5G illumination of the QR arrays covered with aluminium oxide ( $\text{Al}_2\text{O}_3$ ),  $\text{SiN}_x$ ,  $\text{SiO}_2$  and a  $\text{SiO}_2/\text{SiN}_x$  stack [34].

Surface recombination on axial  $p$ - $n$  junction QR arrays has a significant impact on both short circuit current density ( $J_{sc}$ ) and open circuit voltage ( $V_{oc}$ ). Through deep investigation of the effects of different passivations and Si QR lengths as well as effective control of carrier recombination, the efficiency has been recorded as 17.11% on large area ( $125 \times 125 \text{ mm}^2$ ) Si QRSCs by conventional industrial manufacturing processes [34]. This idea opens a potential prospect for the practical fabrication of large size Si QRSCs with satisfactory conversion efficiency.

#### 4.4. Quantum dot solar cells

QD structures have been implemented in various SC applications and it is possible to synthesize QDs in many compositions (semiconductors or metals) as well as coat them with dielectrics or additional semiconductors [1]. One of the early efforts in the utilization of QDs was the down conversion of high-energy photons [36]. The fundamental mechanism of down conversion is the absorption of high-energy photon with relaxation into intermediate states within the bandgap energy, thus emitting two lower energy photons. In a bulk SC, high-energy photons are excited well beyond the CB edge, where they are mostly lost due to interaction with phonons (thermalization). Down conversion aims to absorb these high-energy photons and shift them to lower energies that are matched to specific absorber material in the SC. Several schemes have been proposed to capture and convert the photons to lower energy that are better tuned to the bandgap energy of the semiconductor using nanostructures. One of them formed Si QDs in a dielectric layer deposited on top of a standard Si SC [37]. A small enhancement in quantum efficiency at short wavelengths was observed; however, the overall efficiency was not enhanced. The opposite

of down conversion is the up conversion of photons of energy below the bandgap energy that are typically not absorbed by the bulk SC [38]. The typical mechanism of up conversion involves absorption of sub-bandgap energy light into an intermediate state, followed by further absorption of a second photon to the CB edge. Another novel band structure that can be obtained with QDs is the intermediate band (IB), which is indeed a form of up conversion. This is possible because the states of closely spaced QDs can overlap to form an effective band structure (min-bands) that when finely tuned yields an IB. In the mid-1990s, a new proposal called QD intermediate band SC (QDIBSC) appeared. In this type, the QDs are embedded in a *p-i-n* structure [39]. In addition, another proposal used multi-layered Si QD arrays to create an all Si-based multi-junction SC [40]. The following sub-sections include more details about multi-junctions and IB SCs based on QDs.

#### 4.4.1. Multi-junction solar cells

Wavelengths of the light spectrum from UV to IR cannot be effectively captured by a semiconductor of particular  $E_g$ . If  $E_g$  is too large, most of the photons will not be absorbed; if it is too small, the photons will be absorbed, but much of their energy will be lost by thermalization. To overcome this phenomenon, various techniques have been suggested. One of these techniques is multi-junction SCs (MSCs). The concept of MSCs uses several *p-n* junction SCs with different bandgap energies in tandem which capture efficiently different parts of the light spectrum. The use of different materials in MSCs constitutes a technology challenge because it is very expensive such as GaInP/GaInAs/Ge SC which has achieved 41% efficiency [41]. It is good if one realizes different bandgap energies using only one material such as Si whose bandgap energy is varied using appropriate nanostructures. This idea is behind the all-Si multi-junction tandem SC using different size of QDs nanostructure. **Figure 10** shows this idea as the light comes to the top and the lowest wavelengths are first absorbed whereas the higher wavelengths go through and are absorbed in the middle and bottom cells. There are many ways of realizing such multi-layers. One of the best ways is to deposit alternate thin nanoscale layers of  $\text{SiO}_2$  and a silicon-rich oxide ( $\text{SiO}_x$ ,  $x < 2$ ) [42]. During the annealing, the excess Si in the  $\text{SiO}_x$  layer precipitates to form Si nanocrystals separated by  $\text{SiO}_2$  layers according to the reaction:  $2 \text{SiO}_x = (2 - x)\text{Si} + \text{SiO}_2$ , thus achieving the desired structure. The  $\text{SiO}_x$  layer thicknesses are controlled by varying the deposition time. It is well known that the ground state energies of CCs are raised by the quantum confinement, thus increasing the effective bandgap energy in a nanocrystal compared to the bulk. Further, the smaller the size of the nanocrystal, the larger the bandgap energy. **Figure 11(a)** and (b) shows the pictures of the multi-layer  $\text{SiO}_2/\text{SiO}_x$  structures, and the formation of Si nanocrystals after annealing at  $900^\circ\text{C}$ . Some bandgap energies of the nanocrystals were measured by using the photo-spectrometer. The results showed that the bandgap energy increases as the nanocrystal size decreases. When nanocrystal thickness changed from 2 to 10 nm, the bandgap energy changed from 2.5 to 1.45 eV, respectively [43]. This establishes that the multi-junction tandem SCs can be built with varying the bandgap energies by using only Si and its oxide.

#### 4.4.2. Intermediate band solar cells

QDs super-lattice included in the active region of *p-i-n* single-junction SCs has been considered as one of the candidates to realize the QDIBSCs, as illustrated in **Figure 12**. The IBs allow for the absorption of low-energy photons that would otherwise be transmitted through the bulk

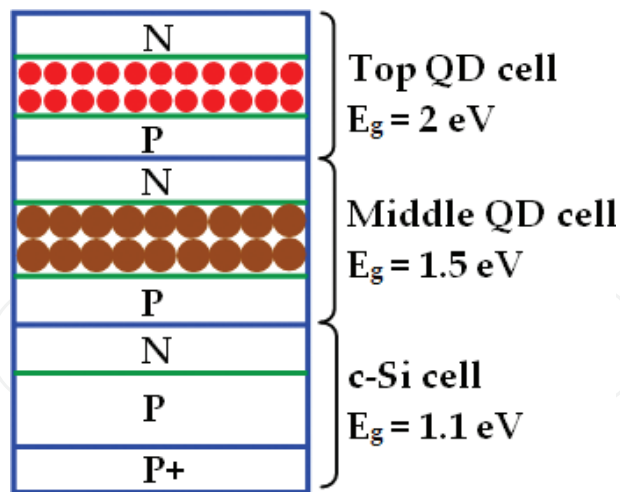


Figure 10. Three junction "all-Si" tandem SC using two layers of Si QDs.

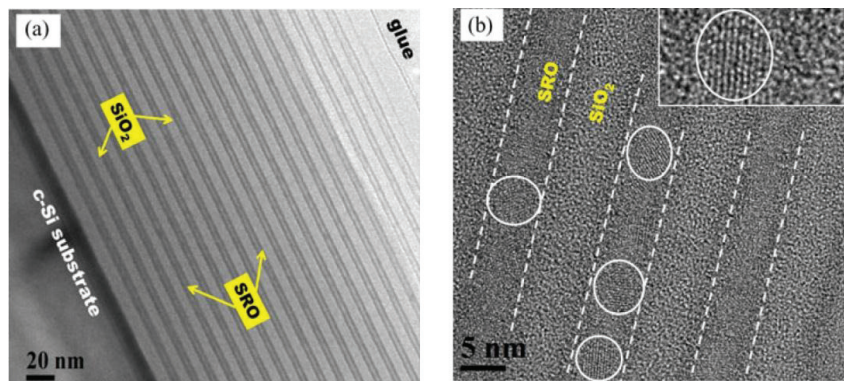


Figure 11. Pictures of 41-layers  $\text{SiO}_2/\text{SiO}_x$  structure before (a) and after (b) annealing [43].

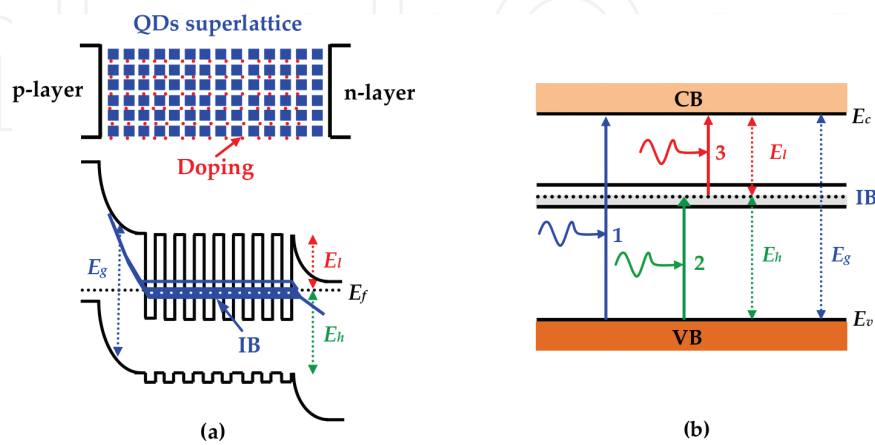
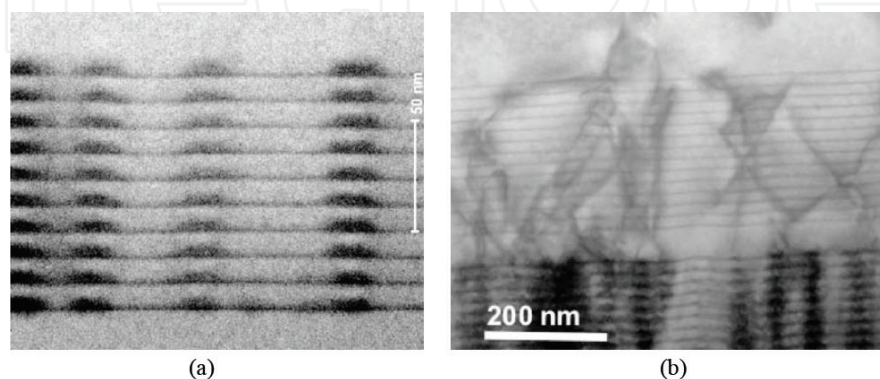


Figure 12. (a) Structure of QDIBSC and energy bands with possible photoabsorption and (b) simplified bandgap energies with three relevant optical transitions [45].

SCs [44]. In the last decade, there has been an extensive effort to demonstrate the QDIBSCs with a central focus on III-V compound semiconductors [45–53]. QDs must be dense to achieve the sufficient photo-absorption in QD layers. QDs are very small and do not absorb much light. Thus, it is necessary to have several layers of QDs. But, these layers cause additional strain and, therefore, the substrate of SC is damaged and performance is reduced. Therefore, the number of QD layers is limited. The typical real density of QDs is the order of  $10^{10}$  per  $\text{cm}^2$  in a single layer for InAs QDs grown on GaAs substrate [47]. For multi-stacked InAs/GaAs SCs with 10 and 50 stacked QDs layers, shown in **Figure 13**, the QDs are vertically aligned in the growth direction without dislocations in 10 stacked QD layers. By contrast, a lot of strain-induced dislocations are observed at both the GaAs substrate and InAs QDs grown regions on sample with 50 stacked QD layers. These defects lead to a significant non-radiative recombination and a reduction in photocurrent productions. Efficiencies of this configuration are now greater than 18%. By using the intermittent deposition technique, ultra-high stacked  $\text{In}_{0.4}\text{Ga}_{0.6}\text{As}/\text{GaAs}$  QDIBSC fabricated [47]. The critical thickness in  $\text{In}_{0.4}\text{Ga}_{0.6}\text{As}/\text{GaAs}$  system is much thicker than in InAs/GaAs system. Therefore,  $\text{In}_{0.4}\text{Ga}_{0.6}\text{As}$  QDs have the advantage of being able to ultra-high stack. In this type, no dislocations are generated after the stacking up to 300 QD layers. They have been successful in the stacking of 400 QD layers while keeping the high crystal quality.

More theoretical calculations have shown that efficiencies of 63% for IBSCs can be achieved under maximum sun concentration and 47% for one sun, which is a significant improvement on the corresponding maximum single junction efficiency of 41% [44–47]. The reason for improvement of the efficiency in QDIBSCs is mainly that the IB formed among QDs increases absorption of longer wavelength region sunlight and reduces non-radiative combination. Recent studies have shown that efficiencies of QDIBSCs can be improved by using different compositions from III-V semiconductor materials [48–53]. It depends essentially on controlling each of the QDs size and the distances between them in the host materials. For example, in reference [48], the authors designed and studied a theoretical model for one intermediate band QDs SC. The composition of both QDs and host materials are  $\text{InAs}_{0.9}\text{N}_{0.1}$  and  $\text{GaAs}_{0.98}\text{Sb}_{0.02}$ , respectively. These studies are based on the Schrödinger equation and it is solved by using the Kronig-Penney model. This work changes the size of QDs and the distance between them, and therefore controls of the location of the IB between the CB and VB. The authors have changed the size of QDs by the values of 8.1, 8.6 and 9.1 nm with the distance between the QDs in the host material constant at 1.98 nm.



**Figure 13.** QDIBSC with 10 QD layers in (a) and 50 QD layers in (b) from InAs grown on GaAs substrate [47].

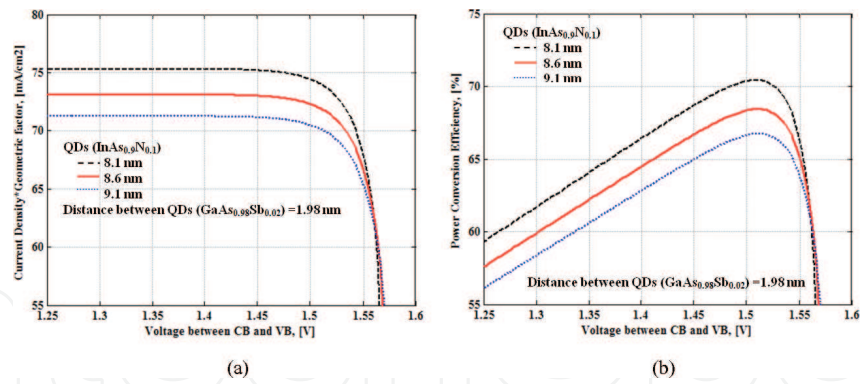


**Figure 14.** Current density in (a) and output power conversion efficiency in (b) for QDIBSC at maximum concentration [48].

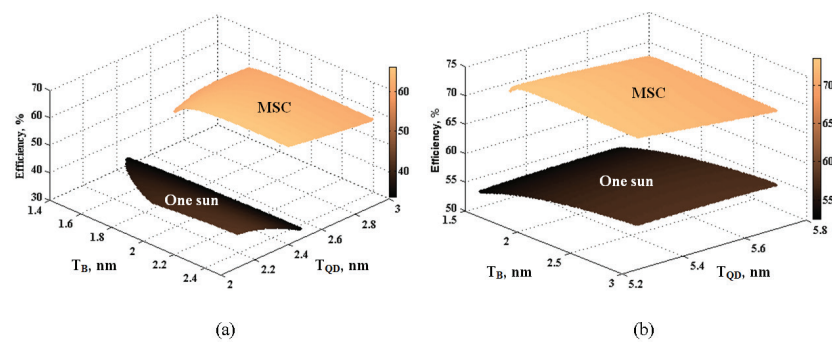


**Figure 15.** Efficiencies versus size of QDs ( $T_{QD}$ ) and distance between QDs ( $T_B$ ) for one IB and two IBs QDSC at one sun and maximum sun concentration (MSC) [53]. One-IB QDSC at one sun and MSC. Two-IBs QDSC at one sun and MSC.

They obtained a relationship between the cell voltage and the output current density from one side and the power conversion efficiency from another side, as shown in **Figure 14(a)** and **(b)**.

From **Figure 14**, it is clear that the current density and efficiency of the cell change inversely with change of the QDs size. The efficiency reached 57.5% and 70.4% at one sun and maximum concentration, respectively [48]. One of the challenges of the QDIBSCs theoretical study is to gather between the one and two IBs in the same time as it is a very complicated issue because some parameters should achieve the physical nanostructure layer concepts. One of the important parameter which should be preserved during theoretical derivation is potential bandgap energy condition. *Aly* and *Nasr* recently studied these cases (one and two IBs) to determine which one will yield highest efficiency [53]. From **Figure 15**, one can notice that the highest efficiency is achieved in the case of two IBs and reached 73.55% at maximum concentration with the following data: size of QDs is 5.25 nm, distance between them is 2.09 nm, and the composition of both QDs and host materials are InAs<sub>0.9</sub>N<sub>0.1</sub> and GaAs<sub>0.98</sub>Sb<sub>0.02</sub>, respectively.

## 5. Conclusions

In this chapter, current attempts for the use of nanostructure materials to improve the performance of SCs have been reviewed. Some of the different ways to reduce the cost and

increase the efficiency of SCs have been summarized. Nanostructures for SCs that have been discussed in this work are nanocomposites, QWs, QRs and QDs. Nanocomposite SCs based on thin films, hot carrier and dye-sensitized structures have shown promising performance in commercial context. Nanostructured layers in thin film SCs offer a number of important advantages such as the effective optical path for absorption is much larger than the actual film thickness, recombination losses are greatly reduced, the absorber layer thickness can be as thin as 150 nm and thus installation costs can be reduced and finally, reduced manufacturing costs as a result of using a low temperature process. The performance of hot carrier SCs improves when the absorber layer is QDs superlattice. For dye-sensitized SCs, the wide-bandgap energy semiconductors such as  $\text{TiO}_2$  and CNT fibres in the form of nanoparticles have been used to maximize the contact area between them and the dye. The presence of QW in the depletion layer of SCs produces electric field that leads to the collection of charge carriers photo-generated in the wells, leading to an enhanced current. The efficiency of this type is improved when the number of QWs increases. QRs SCs improve the performance and reduce the cost based on increased absorption due to diffuse light scattering in QR arrays, short collection lengths of minority carriers and flexibility of cell integration on a variety of low-cost carrier substrates. Finally, QDs have been shown to be useful in SC devices in various modes such as multi-layered QD arrays and QDIBSCs. The efficiency for multi-junction achieved is 41%. Nanostructures are used to realize different bandgap energies using only one material such as Si to reduce the cost. Therefore, all-Si multi-junction tandem SCs can be produced by using different size nanocrystals or QDs from Si. The QDIBSCs are one of the most promising candidates to improve and enhance the performance of SCs. More theoretical studies for this type were carried by using different compositions from III-V semiconductor materials. In fact, these studies showed that the performance of this type depends largely on the compositions of materials, size of QDs and the distance between them in the host materials. The theoretical efficiency in these SCs reached as high as 73.55%.

## Author details

Abouelmaaty M. Aly

Address all correspondence to: [abouelmaaty67@gmail.com](mailto:abouelmaaty67@gmail.com)

1 Electronic Research Institute, Cairo, Egypt

2 College of Computer, Qassim University, Buryadah, Kingdom of Saudi Arabia

## References

- [1] Tsakalakos L: Nanostructures for photovoltaics. *Materials Science and Engineering R*. 2008; 62: 175-189. DOI: 10.1016/j.mser.2008.06.002
- [2] Shockley W, Queisser H. J: Detailed balance limit of efficiency of p-n junction solar cells. *Journal of Applied Physics*. 1961; 32(3): 510-519. DOI: 10.1063/1.1736034

- [3] Singh J: Electronics and Optoelectronic Properties of Semiconductor Structures. 1<sup>st</sup> ed. Cambridge, UK: Cambridge University Press; 2003. 288 p. DOI: 10.2277/052182379X
- [4] Nayfeh M O, et al.: Thin film silicon nanoparticle UV photodetector. IEEE Photonics Technology. 2004; 16(8): 1927-1929. DOI: 10.1109/LPT.2004.831271
- [5] Aly M A: Improving the Power Conversion Efficiency of the Solar Cells. Qassim University Journal of Engineering and Computer Sciences. 2014; 7(2): 135-156. <http://publications.qu.edu.sa/ojs/index.php/engineering/article/view/1399>
- [6] Zhang G, et al.: Semiconductor nanostructure-based photovoltaic solar cells. Nanoscale. 2011; 3(6): 2430-2443. DOI: 10.1039/C1NR10152H
- [7] Zhang Q, Gao G: Nanostructured photoelectrodes for dye-sensitized solar cells. Nanotoday. 2011; 6(1): 91-109. DOI: 10.1016/j.nantod.2010.12.007
- [8] Zhu J, et al.: Optical absorption enhancement in amorphous silicon nanowire and nanocone arrays. Nano Lett. 2009; 9(1): 279-282. DOI: 10.1021/nl802886y
- [9] Kibria T M, et al.: A review: Comparative studies on different generation solar cells technology. In: Proceedings of 5<sup>th</sup> International Conference on Environmental Aspects of Bangladesh (ICEAB); 5-6 September 2014; Dhaka. Bangladesh; 2014. pp. 51-53.
- [10] Ojajarvi J: Tetrahedral chalcopyrite quantum dots in solar cell applications [thesis]. Department of Physics: University of Jyvaskyla; 2010.
- [11] Javawardena G D K, et al.: Inorganics-in-organics: recent developments and outlook for 4G polymer solar cells. Nanoscale. 2013; 5: 8411-8427. DOI: 10.1039/C3NR02733C
- [12] Kasap S, Capper P: Springer Handbook of Electronic and Photonic Materials. In: Fox M, Ispasoiu R, editors. Quantum Wells, Superlattices and Band-Gap Engineering. 2<sup>nd</sup> ed. Springer:NY, US; 2007. pp. 1021-1040. DOI: 10.1007/978-3-319-48933-9.ch42
- [13] Morozhenko V: Infrared Radiation. In: Nasr A, editor. Infrared Radiation Photodetectors. InTech:Rijeka, Croatia; 2012. pp. 85-126. DOI: 10.5772/2031.ch5
- [14] Soga T: Nanostructured Materials for Solar Energy Conversion. 1<sup>st</sup> ed. Elsevier B. V.: Amsterdam, Netherlands; 2006. 485 p. DOI: 10.1016/B978-044452844-5/50000-7
- [15] Deng Q, et al.: Theoretical study on  $\text{In}_x\text{Ga}_{1-x}\text{N}/\text{GaN}$  quantum dots solar cell. Physica B. 2011; 406(1): 73-76. DOI: 10.1016/j.physb.2010.10.020
- [16] Singha R, et al.: Nanostructured CdTe, CdS and  $\text{TiO}_2$  for thin film solar cell applications. Solar Energy Materials & Solar Cells. 2004; 82(1): 315-330. DOI: 10.1016/j.solmat.2004.02.006
- [17] Nabhani N, Emami M: Nanotechnology and its Applications in Solar Cells. In: 2<sup>nd</sup> International Conference on Mechanical and Industrial Engineering (ICMIE'2013); 8-9 March 2013; Kota Kinabalu. Malaysia; 2013. pp. 88-91.

- [18] König D, et al.: Hot carrier solar cells: principles, materials and design. *Physica E: Low-dimensional Systems and Nanostructures*. 2010; 42(10): 2862-2866. DOI: 10.1016/j.physe.2009.12.032
- [19] Zhang Y, et al.: Development of inorganic solar cells by nanotechnology. *Nano-Micro Lett.* Springer Berlin Heidelberg, Germany. 2012; 4(2): 124-134. DOI:10.1007/BF03353703
- [20] Conibeer J G, et al.: Slowing of carrier cooling in hot carrier solar cells. *Thin Solid Films*. 2008; 516(20): 6948-6953. DOI: 10.1016/j.tsf.2007.12.102
- [21] Aliberti P, et al.: Investigation of theoretical efficiency limit of hot carriers solar cells with a bulk indium nitride absorber. *Journal of Applied Physics*. 2010; 108(094507): 1-10. DOI:10.1063/1.3494047
- [22] Grätzel M: Dye-sensitized solar cells. *Journal of Photochemistry and Photobiology C: Photochemistry Reviews*. 2003; 4(2): 145-153. DOI: 10.1016/S1389-5567(03)00026-1
- [23] Wang P, et al.: A stable quasi-solid-state dye-sensitized solar cell with an amphiphilic ruthenium sensitizer and polymer gel electrolyte. *Nature Materials*. 2003; 2: 402-407. DOI:10.1038/nmat904
- [24] Yang J H, et al.: Characteristics of the dye-sensitized solar cells using TiO<sub>2</sub> nanotubes treated with TiCl<sub>4</sub>. *Materials*. 2014; 7(5): 3522-3532. DOI:10.3390/ma7053522
- [25] Alturaif H A, et al.: Use of carbon nanotubes (CNTs) with polymers in solar cells. *Molecules*. 2014; 19: 17329-17344. DOI:10.3390/molecules191117329
- [26] Zhang Y, et al.: Improved dye-sensitized solar cell performance in larger cell size by using TiO<sub>2</sub> nanotubes. *Nanotechnology*. 2013; 24(4): 045401-6. DOI:10.1088/0957-4484/24/4/045401
- [27] Carlos I. Cabrera, et al.: Modeling multiple quantum well and superlattice solar cells. *Natural Resources*. 2013; 4: 235-245. DOI: 10.4236/nr.2013.43030
- [28] Carlos I. Cabrera, et al.: Modelling of GaAsP/InGaAs/GaAs strain-balanced multiple-quantum well solar cells. *Journal of Applied Physics*. 2013; 113(024512): 1-7. DOI: 10.1063/1.4775404
- [29] Yang M, Yamaguchi M: Properties of GaAs/InGaAs quantum well solar cells under low concentration operation. *Solar Energy Materials and solar Cells*. 2000; 60(1): 19-26. DOI: 10.1016/S0927-0248(99)00055-0
- [30] Garnett E C, et al.: Nanowire solar cells. *Annual Review of Materials Research*. 2011; 41: 269-295. DOI: 10.1146/annurev-matsci-062910-100434
- [31] Tsakalakos L, et al.: Silicon nanowire solar cells. *Applied Physics Letters*. 2007; 91: 233117-1 to 3. DOI: 10.1063/1.2821113
- [32] Srivastava S K, et al.: Excellent anti-reflection properties of vertical silicon nanowire arrays. *Solar Energy Materials and Solar Cells*. 2010; 94(9): 1506-1511. DOI: 10.1016/j.solmat.2010.02.033

- [33] Kim J Y, et al.: Postgrowth in situ chlorine passivation for suppressing surface-dominant transport in silicon nanowire devices. *IEEE Transactions Nanotechnology*. 2012; 11(4): 782-787. DOI: 10.1109/TNANO.2012.2197683
- [34] Anna D M: Nanowire-based solar cells: Device design and implementation [thesis]. Ecole Polytechnique Federale de Lausanne, Suisse; 2014.
- [35] Kerr M J, Cuevas A: General parameterization of auger recombination in crystalline silicon. *Journal of Applied Physics*. 2002; 91: 2473-2480. DOI: 10.1063/1.1432476
- [36] Trupke T, et al.: Improving solar cell efficiencies by down-conversion of high-energy photons. *Journal of Applied Physics*. 2002; 92: 1668-1674. DOI: 10.1063/1.1492021
- [37] Svrcek V, et al.: Silicon nanocrystals as light converter for solar cells. *Thin Solid Films*. 2004; 451(3): 384-388. DOI: 10.1016/j.tsf.2003.10.133
- [38] Shalav A, et al.: Luminescent layers for enhanced silicon solar cell performance: up-conversion. *Solar Energy Materials and Solar Cells*. 2007; 91(9): 829-842. DOI: 10.1016/j.solmat.2007.02.007
- [39] Marti A, et al.: Production of photocurrent due to intermediate-to-conduction-band transitions: a demonstration of a key operating principle of the intermediate-band solar cell. *Physics Review Letters*. 2006; 97(24): 247701-247704. DOI: 10.1103/PhysRevLett.97.247701
- [40] Green M A, et al.: Nanostructured Silicon-Based Tandem Solar Cells [Project]. Sydney, Australia: University of New South Wales; 2005.
- [41] Cho E-C, et al.: Silicon quantum dot/crystalline silicon solar cells. *Nanotechnology*. 2008; 19(24): 245201. DOI: 10.1088/0957-4484/19/24/245201
- [42] Mavilla N R, et al.: Structural properties of ICPCVD fabricated SiO<sub>2</sub>/SiO<sub>x</sub> superlattice for use in beyond Shockley-Queisser-limit solar cells. In: 27th European Photovoltaic Solar Energy Conference (EUPVSEC); 24-28 September 2012; Frankfurt. Germany; 2012. pp. 379-381.
- [43] Rao M N, Solanki C S and Vasi J: Nanotechnology for next generation photovoltaics. In: 82nd Annual Symposium of NASI on "Nano-science and technology for Mankind"; 2012; Varanasi. India; 2012. pp. 340-350.
- [44] Luque A, et al.: Increasing the efficiency of ideal solar cells by photon induced transitions at intermediate levels. *Physics Review Letters*. 1997; 78: 5014-5017. DOI: 10.1103/PhysRevLett.78.5014
- [45] Nasr A, Aly A M. Performance evaluation of quantum-dot intermediate-band solar cell. *Journal of Electronic Materials*. 2016; 45(1): 672-681. DOI: 10.1007/s11664-015-4172-z
- [46] Okada Y, et al.: Intermediate band solar cells: recent progress and future directions. *Applied Physics Reviews*. 2015; 2: 021302-1 to 48. DOI: 10.1063/1.4916561
- [47] Martí A, et al.: Emitter degradation in quantum dot intermediate band solar cells. *Applied Physics Letters*. 2007; 90(233510): 6233-6237. DOI: 10.1063/1.2747195

- [48] Aly A. M, Nasr A: Theoretical performance of solar cell based on minibands quantum dots. *Journal of Applied Physics*. 2014; 115(114311): 114311-1 to 114311-9. DOI: 10.1063/1.4868982
- [49] Aly A, Nasr A: Theoretical study of one-intermediate band quantum dots solar cell. *International Journal of Photoenergy*:2014; 2014(904104): 1-10. DOI: 10.1155/2014/904104
- [50] Aly A M: Progress into power conversion efficiency for solar cells based on nanostructured and realistic spectra. *Journal of Renewable Sustainable Energy*. 2014; 6(023118): 023118-1 to 023118-9. DOI: 10.1063/1.4873132
- [51] Nasr A, Aly A: Theoretical investigation of some parameters into the behavior of quantum dot solar cells. *Journal of Semiconductor*. 2014; 35(12): 124001-8. DOI: 10.1088/1674-4926/35/12/124001
- [52] Aly A M: Investigation of some parameters which affects into the efficiency of quantum dot intermediate band solar cell. *International Journal of Renewable Energy Research*. 2014; 4(4): 1085-1093. <http://www.ijrer.org/ijrer/index.php/ijrer/article/view/1714>
- [53] Aly A, Nasr A: The effect of multi-intermediate bands on the behavior of an  $\text{InAs}_{1-x}\text{N}_x/\text{GaAs}_{1-y}\text{Sb}_y$  quantum dot solar cell. *Journal of Semiconductor*. 2015; 36(4): 042001-6. DOI: 10.1088/1674-4926/36/4/042001

